

# Verifiable Evaporation Modeling on the Laurentian Great Lakes

THOMAS E. CROLEY II

*Great Lakes Environmental Research Laboratory, Environmental Research Laboratories, National Oceanic and Atmospheric Administration, U.S. Department of Commerce, Ann Arbor, Michigan*

Water or energy balance estimates of Great Lakes evaporation require storage change data, not available in simulations or forecasts, and errors in the components of the balances are summed in the residual, giving large estimation errors. Neither these balance estimates nor evaporation models, which use the aerodynamic equation with mass transfer coefficients developed originally in the Lake Hefner studies, can be verified, since independent estimates of evaporation are not available with sufficient accuracy. However, water surface temperatures can be used to verify energy budgets. The mass transfer coefficient research is combined here with lumped concepts of classical energy conservation and a new superposition heat storage model to provide continuous simulation capability of both water surface temperatures and lake evaporation for use in outlooks and forecasts of lake levels. Calibration matches remotely sensed water surface temperatures for those Great Lakes with observations over the past 20 years. Model sensitivities are analyzed and heat and water budgets are compared.

## INTRODUCTION

Understanding short- and long-term variations in the Laurentian Great Lakes water levels and the hazards associated with them requires lake level forecasts and simulations, both of which have lake evaporation modeling as an integral part. As lake evaporation for the Great Lakes is on the same order of magnitude as precipitation and runoff to the lakes, it represents a significant component of the Great Lakes hydrologic cycle, and its determination is crucial in estimating lake levels. Evaporation determination for large lakes is still difficult even after years of research due to the unavailability of pertinent data over large areas, the complexity of the evaporation process, and the present lack of understanding of heat storage in large lakes. The Great Lakes Environmental Research Laboratory (GLERL) had been using evaporation estimates from the aerodynamic equation with stability-dependent mass transfer coefficients developed during the International Field Year on the Great Lakes (IFYGL) for Lake Ontario and modified for other lakes. Unfortunately, there have been no really good independent evaporation data to verify this approach on the Great Lakes. Water balance determinations are insufficient due to the large errors introduced by subtracting nearly equal large inflows and outflows to each Great Lake but Superior. Even on Lake Superior, with its relatively smaller inflows and outflows, the water balance allows only a crude comparison. Energy balances also suffer by summing errors in all terms into the residual evaporation estimate.

Since uses of the aerodynamic equation and of energy balance techniques require knowledge of surface temperatures, a second problem is that these uses are not amenable to use in forecast settings (where future surface temperatures are unknown). It is necessary to model both the heat storage and the evaporation process (through consideration of the heat balance and surface temperature) to enable extrapolation of surface temperatures for forecasting evaporation. Until recently, such consideration was not possible, since surface temperatures have not been widely available

This paper is not subject to U.S. copyright. Published in 1989 by the American Geophysical Union.

Paper number 89WR00247.

for calibration of such a model. Now, remotely sensed historical surface temperatures are available for all Great Lakes except Michigan, forming an independent data set that may be used for comparisons in evaporation heat balances and model verification.

To take advantage of the newly available surface temperature data, to allow recognition of meteorological variability filtered by monthly averaging, and to remain consistent with other Great Lakes hydrology models, a daily evaporation model is desired for use over the lake surface. To avoid additional computational burden inappropriate for long simulations, calibrations, or real-time forecasts and to maintain model sophistication in line with data availability, a spatially lumped model of the entire lake surface is constructed. As a first effort, a new one-dimensional concept of heat storage is combined here with existing spatially lumped models (where water temperatures must be known) of the heat balance and evaporation process to estimate Great Lakes evaporation efficiently in simulation and forecast settings. The resulting model is calibrated with surface temperatures for four of the Great Lakes and Lake St. Clair and compared to existing evaporation estimates.

## GREAT LAKES EVAPORATION MODEL

Great Lakes evaporation studies typically used mass transfer formulations from the classic Lake Hefner study [U.S. Geological Survey, 1954, 1958] [see Richards and Irbe, 1969]. More recently, Phillips [1978] and Quinn [1979] included atmospheric stability effects on Great Lakes evaporation bulk transfer coefficients; the latter approach is used presently by both Canadian and U.S. agencies applied to monthly data for surface temperatures, wind speed, humidity, and air temperatures [Derecki, 1981; Quinn and Kelley, 1983; Atmospheric Environment Service (AES), 1988]. That approach is outlined here for convenience [after Quinn, 1979].

### Bulk Evaporation Coefficient

Paulson [1970] summarized the application of Monin and Obukhov's similarity hypothesis to field measurements of wind speed and air temperature in the atmospheric surface

layer (in which turbulent fluxes are taken as constant with height). Following *Panofsky* [1963] and *Businger* [1966], he established wind and temperature profiles respectively as

$$U = U_* k^{-1} [\ln (Z/Z_w) - S_1] \quad (1)$$

$$T - T_w = T_* [\ln (Z/Z_w) - S_2] \quad (2)$$

where  $U$  is mean wind speed at reference height  $Z$  above the surface,  $U_*$  is the friction velocity,  $k$  is von Karmán's constant,  $Z_w$  is the roughness length,  $T$  is the potential temperature at reference height,  $T_w$  is the potential temperature at  $Z_w$ ,  $T_*$  is the scaling temperature, and

$$T_* = Q_h / (r C_p k U_*) \quad (3)$$

$$S_1 = 2 \ln \{ [1 + (1 - a_1 Z/L)^{1/4}] / 2 \} + \ln \{ [1 + (1 - a_1 Z/L)^{1/2}] / 2 \} \\ - 2 \tan^{-1} (1 - a_1 Z/L)^{1/4} + 1.570796 \quad Z/L \leq 0$$

$$= -a_2 Z/L \quad 0 < Z/L < 1 \\ = -a_2 [1 + \ln (Z/L)] \quad Z/L \geq 1 \quad (4)$$

$$S_2 = 2 \ln \{ [1 + (1 - a_3 Z/L)^{1/2}] / 2 \} \quad Z/L \leq 0 \\ = -a_2 Z/L \quad 0 < Z/L < 1$$

$$= -a_2 [1 + \ln (Z/L)] \quad Z/L \geq 1 \quad (5)$$

where  $Q_h$  is the turbulent heat flux to the surface,  $r$  is the air density,  $C_p$  is the specific heat of air at constant pressure,  $S_1$  and  $S_2$  are the stability-dependent parameters for the wind and temperature profiles, respectively, and

$$L = U_*^{-3} C_p r Y / (k g Q_h) \quad (6)$$

where  $L$  is the Monin-Obukhov length,  $Y$  is the absolute temperature of near-surface air, and  $g$  is the acceleration due to gravity. Note from (4) and (5) that wind speed and air temperature are functions of the stability parameter,  $Z/L$ , where  $Z/L < 0$  denotes unstable conditions,  $Z/L = 0$  is neutral,  $0 < Z/L < 1$  is stable, and  $Z/L \geq 1$  is strongly stable.

*Quinn* [1979] used *Charnock's* [1955] relationship for neutral conditions over a large surface to obtain

$$Z_w = a_4 U_*^2 / g \quad (7)$$

By taking the bulk evaporation coefficient  $C_E$  equal to the sensible heat coefficient  $C_H$ ,

$$C_E = C_H \quad (8)$$

*Quinn* [1979] used turbulent heat flux (written here as to the lake surface)

$$Q_h = r C_p C_H (T - T_w) U \quad (9)$$

and (1)–(7) to derive an expression for  $C_E$  so that evaporation over water  $E_w$  can be expressed as an equivalent depth by the bulk aerodynamic evaporation formulation

$$E_w = r C_E (q_w - q) U / r_w \quad (10)$$

where  $q$  is the specific humidity of the atmosphere,  $q_w$ , the saturation specific humidity at the surface temperature, and  $r_w$ , the density of water.

Equations (1) through (10) may be solved simultaneously to determine evaporation from  $U$ ,  $T$ ,  $T_w$  (taken as surface

temperature),  $q_w$ , and  $q$ . *Quinn* [1979] solved them for his computations of overlake evaporation on Lake Ontario with monthly data taken during IFYGL. He chose empirical coefficients,  $a_1 = 16$ ,  $a_2 = 5.2$ ,  $a_3 = 16$ , and  $k = 0.41$  as best representing the atmospheric surface layer and determined  $a_4 = 0.0101$  by using observations of his own. He also used  $Z = 8$  m,  $g = 9.8$  m s<sup>-2</sup>, and constant  $Y = 276.5^\circ\text{K}$  (since normal variations in  $Y$  make little difference in  $L$ ); these eight values are used herein.

### Overwater Meteorology

As overwater data are not available generally, overland data are used with correction for overwater conditions. *Phillips and Irbe* [1978] studied overwater data available from specially placed data buoys on Lake Ontario during IFYGL and, in step-wise multiple linear regressions, related overwater data to air stability (indexed by the overland air temperature minus the surface temperature), fetch length in the wind direction, overland wind speed, duration of air over water, overland air temperature, surface temperature, and overland dew point temperature. Their regressions for overwater corrections are used here by replacing the fetch (and derived quantities) with averages over the data set for each stability class, similar to other efforts [*Derecki*, 1981]:

$$U = b_0 + b_1 W + b_2 T_a + b_3 T_w \quad (11)$$

$$T = b_4 + b_5 T_a + b_6 T_w \quad (12)$$

$$D = b_7 + b_8 T_w + b_9 D_1 \quad (13)$$

where  $U$  is expressed in meters per second;  $W$  is the overland wind speed (meters per second);  $T_a$  is the overland air temperature ( $^\circ\text{C}$ );  $T_w$  and  $T$  are expressed in  $^\circ\text{C}$ ;  $D$  and  $D_1$  are the overwater and overland dew point temperatures, respectively ( $^\circ\text{C}$ ); and  $b_0, \dots, b_9$  are empirical coefficients for a given lake and stability class (range of the air-water temperature difference,  $T_a - T_w$ ). The empirical coefficients for (11), (12), and (13) are given in Table 1.

### Ice Cover

As the lakes experience significant ice cover during the winter season, the estimated evaporation must be corrected for the effects of ice. This is done here by using temperatures and specific humidities over ice for the overice evaporation calculation in (10) and over water for the overwater calculations; the two estimates are then combined by weighting for the fraction of the surface covered in ice. Existing data on ice cover [*Assel*, 1983] were used to determine empirical relations between ice cover extent and air temperatures, similar to other efforts [*Derecki*, 1981]:

$$I = \max (\min (c_1 - c_2 Y_a - c_3 Y_{a-1}, 1.0), 0.0) \quad (14)$$

where  $I$  is the monthly average fraction of the surface covered by ice,  $c_1$ ,  $c_2$ , and  $c_3$  are empirical coefficients for a given lake and month,  $Y_a$  is the monthly average overland air temperature ( $^\circ\text{C}$ ), and  $Y_{a-1}$  is the monthly average overland air temperature ( $^\circ\text{C}$ ) for the previous month. The empirical coefficients for (14) are given in Table 2.

### HEAT STORAGE

*Gill and Turner* [1976] applied *Kraus and Turner's* [1967] mixed-layer concept in a lumped representation to North

TABLE 1. Overwater Meteorology Coefficients,  $b_i$

| Stability Class                              | $b_0$ | $b_1$ | $b_2$ | $b_3$ | $b_4$  | $b_5$ | $b_6$ | $b_7$  | $b_8$ | $b_9$ |
|--|-------|-------|-------|-------|--------|-------|-------|--------|-------|-------|
| <i>All Great Lakes Except Lake St. Clair</i> |       |       |       |       |        |       |       |        |       |       |
| ( $\infty, -10.5$ )                          | 3.132 | 1.05  |       |       | -1.333 | 0.60  | 0.54  | -4.499 | 0.46  | 0.56  |
| $[-10.5, -3.5]$                              | 2.795 | 1.01  |       |       | -0.321 | 0.67  | 0.42  | 0.484  | 0.11  | 0.94  |
| $[-3.5, 3.5]$                                | 1.607 | 0.92  | -0.28 | 0.28  | 0.290  | 0.47  | 0.52  | -0.350 | 0.31  | 0.72  |
| $[3.5, 10.5]$                                | 2.740 | 0.49  | -0.02 |       | 1.485  | 0.29  | 0.65  | -0.160 | 0.55  | 0.44  |
| $[10.5, \infty)$                             | 3.374 | 0.32  | -0.02 |       | 1.822  | 0.30  | 0.56  | -0.037 | 0.53  | 0.43  |
| <i>Lake St. Clair</i>                        |       |       |       |       |        |       |       |        |       |       |
| ( $\infty, -10.5$ )                          | 2.640 | 1.05  |       |       | -2.034 | 0.60  | 0.54  | -5.115 | 0.46  | 0.45  |
| $[-10.5, -3.5]$                              | 2.350 | 1.01  |       |       | -0.696 | 0.67  | 0.42  | 0.240  | 0.11  | 0.94  |
| $[-3.5, 3.5]$                                | 1.141 | 0.92  | -0.28 | 0.28  | 0.290  | 0.47  | 0.52  | -0.350 | 0.31  | 0.72  |
| $[3.5, 10.5]$                                | 2.687 | 0.49  | -0.02 |       | 2.110  | 0.29  | 0.65  | -0.160 | 0.55  | 0.44  |
| $[10.5, \infty)$                             | 3.317 | 0.32  | -0.02 |       | 2.945  | 0.30  | 0.56  | 0.790  | 0.53  | 0.43  |

Data from Croley [1989]. Stability classes are intervals for the air-water temperature difference,  $T_a - T_w$ .

Atlantic sea conditions. It is extended here for the Great Lakes where spring turnover (convective mixing of deep cold low-density water with cool high-density surface waters) occurs when surface temperature increases to 3.98°C, the temperature for maximum density of water. As water temperatures begin increasing above 3.98°C, surface temperature increases faster than temperatures at depth, until a

stable temperature-depth profile develops with warmer, lower-density waters on top. As the net heat flux to the surface then changes to negative, surface temperature drops and convective mixing keeps an upper layer at uniform temperature throughout (the "mixed layer"). The mixed layer deepens until the temperature is uniform over the entire depth at 3.98°C, representing fall turnover. Then a symmetrical behavior is observed with temperatures less than 3.98°C as the lake continues to lose heat; the surface temperature drops the most until the net heat flux at the surface changes to positive again. Surface temperature then increases toward 3.98°C and convective mixing forces uniform temperature at all depths, representing spring turnover.

TABLE 2. Ice Cover Coefficients,  $c_i$

| Month            | $c_1$     | $c_2, ^\circ\text{C}^{-1}$ | $c_3, ^\circ\text{C}^{-1}$ |
|------------------|-----------|----------------------------|----------------------------|
| <i>Superior</i>  |           |                            |                            |
| Jan.             | -0.314387 | -0.012352                  | -0.027498                  |
| Febr.            | -0.455670 | -0.008526                  | -0.045248                  |
| March            | -0.404057 | 0.006066                   | -0.072318                  |
| April            | 0.201811  | -0.028747                  | -0.000638                  |
| Dec.             | -0.028608 | -0.004238                  | 0.000910                   |
| <i>Huron</i>     |           |                            |                            |
| Jan.             | -0.035293 | -0.015755                  | -0.016502                  |
| Febr.            | -0.18775  | -0.031164                  | -0.048973                  |
| March            | -0.13003  | -0.032276                  | -0.060014                  |
| April            | 0.230864  | -0.021162                  | -0.06788                   |
| Dec.             | 0.0       | 0.0                        | 0.0                        |
| <i>Erie</i>      |           |                            |                            |
| Jan.             | 0.0400    | -0.05361                   | -0.05867                   |
| Febr.            | 0.5286    | -0.03375                   | -0.01885                   |
| March            | 0.2272    | -0.04713                   | -0.06002                   |
| April            | 0.1133    | -0.00266                   | -0.018                     |
| Dec.             | 0.0896    | -0.0234                    | -0.01518                   |
| <i>Michigan</i>  |           |                            |                            |
| Jan.             | -0.108262 | -0.016680                  | -0.012855                  |
| Febr.            | -0.116667 | -0.017650                  | -0.018551                  |
| March            | -0.011612 | 0.001294                   | -0.010892                  |
| April            | -0.000429 | 0.004148                   | -0.011771                  |
| Dec.             | 0.001165  | -0.004570                  | -0.007143                  |
| <i>St. Clair</i> |           |                            |                            |
| Jan.             | 0.4091    | -0.05918                   | -0.01517                   |
| Febr.            | 0.6303    | -0.0420                    | -0.02145                   |
| March            | 0.3829    | -0.1042                    | -0.06507                   |
| April            | 0.5122    | -0.0717                    | -0.04211                   |
| Dec.             | 0.2329    | -0.08165                   | -0.04300                   |
| <i>Ontario</i>   |           |                            |                            |
| Jan.             | -0.0586   | -0.018725                  | 0.000276                   |
| Febr.            | -0.14067  | -0.0313                    | -0.016876                  |
| March            | -0.081346 | 0.004778                   | -0.03738                   |
| April            | -0.000144 | 0.007138                   | 0.012394                   |
| Dec.             | 0.0       | 0.0                        | 0.0                        |

Data from Croley [1989].

There is hysteresis in the heating and cooling cycles of the lakes, since the relationship between stored heat and surface temperature is different during these cycles. As surface temperature climbs through the spring turnover, heat in the lake is increasing relatively quickly with surface temperature but this rate soon decreases since mainly surface waters are affected; as temperature approaches its peak, heat in the lake begins increasing more quickly with surface temperature again, as heat migrates down from the surface. After the surface temperature peaks and begins to drop, the heat in the lake continuously slows its ascent until it peaks slightly later than did the temperature. As the lake then begins cooling, heat changes (drops) more and more quickly with (dropping) surface temperature since successively deeper layers are involved in the convective mixing and the lake approaches fall turnover (heat approaches capacity at turnover). Likewise, similar behavior is observed after the fall turnover between the heat deficiency (heat capacity at turnover minus the heat stored) and surface temperature.

After the spring turnover then (or anytime surface temperature is above 3.98°C), if heat is added uniformly throughout a surface layer of depth  $y$ , we can write heat additions as a function of (surface) temperature for daily additions:

$$H_j - H_{j-1} = r_w CA (-y/2)(T_j - T_{j-1})y \quad H_j \geq H_{j-1} \geq H_d \quad (15)$$

where  $H_j$  is the heat in storage in the lake at the end of day  $j$  ( $j$  days after the last spring turnover),  $C$  is the specific heat of water,  $A(Z)$  is the area of the horizontal plane at height  $Z$  above the water surface,  $T_j$  is the surface temperature ( $T_w$ ) at the end of day  $j$ , and  $H_d$  is the heat in storage at turnover

(when the surface temperature, and temperatures at all depths, are 3.98°C). More generally, heat additions penetrate nonuniformly to various depths and for the prismatic case (in which the lake is treated as a cylinder over the penetration depth,  $A(Z) = A$ ,  $0 \leq Z \leq -y$ ):

$$H_j = H_{j-1} + a(T_j - T_{j-1})^c \quad T_j \geq T_{j-1} \geq T_d \quad (16)$$

where  $a$  and  $c$  are empirically derived parameters and  $T_d$  is the temperature of maximum water density (3.98°C). Old heat additions continue penetration (through processes of conduction, diffusion, and mechanical mixing while temperatures are increasing); their effect on surface temperature rise diminishes and an aging function can reflect this:

$$H_m = H_{m-1} + a[1 + b(j-m)^x](T_m - T_{m-1})^c \quad (17)$$

$$0 < m \leq j$$

where  $H_0 = H_d$ ,  $T_0 = T_d$ , and  $b$  and  $x$  are empirically derived parameters. Temperature increments from past heat additions are "added" by superimposing the effects of past daily heat additions to determine the surface temperature. An alternate expression of this superposition can be made in terms of the surface temperature. For the case of continuous heat additions every day, repeated application of (17) gives

$$T_j = T_0 + \sum_{m=1}^j \left\{ \frac{1}{a} (H_m - H_{m-1}) [1 + b(j-m)^x] \right\}^{1/c} \quad (18)$$

If heat is removed, it comes from the surface layers, lowering surface and near-surface temperatures which results in convective mixing (lower-density waters at depth rise) and a deepening of the mixed layer. The most recent heat additions are arbitrarily removed first since they are most available for release (they are less distributed with depth than older additions and have their major fraction closest to the surface). The  $m$ th heat addition is removed (by replacing  $H_m - H_{m-1}$  with zero in equation (18)) when the current heat in storage,  $H_j$ , drops below the  $m$ th ( $H_m > H_j$ ). More generally, heat is added, then removed, then added, and so forth and while recent additions may be lost, new additions will occur. For the general case, in which heat additions and losses may follow one another, (18) becomes

$$T_j = T_0 + \sum_{m=1}^j \left\{ \frac{1}{a} \left( \min_{m \leq n \leq j} H_n - \min_{m-1 \leq n \leq j} H_n \right) \div [1 + b(j-m)^x] \right\}^{1/c} \quad (19)$$

where

$$\min_{m \leq n \leq j} H_n = \min (H_m, H_{m+1}, \dots, H_{j-1}, H_j) \quad (20)$$

A symmetrical expression for heat losses, similar to (19), can be derived for surface temperatures below  $T_d$  (after fall turnover) but experience shows that the use of the same equation for all variations of heat and temperature (no superposition) is adequate:

$$H_j = H_d - a'[1 + b'j^{x'}](T_d - T_j)^{c'} \quad (21)$$

where  $a'$ ,  $b'$ ,  $c'$ , and  $x'$  are empirically derived parameters and  $j$  is measured from the day of the fall turnover.

In the use of (19) and (21), as well as in the estimation of their parameters (calibration), a limit is placed on the effect of aging; after 182 days (arbitrarily chosen) the aging function,  $1 + b(j-m)^x$ , is taken as constant. Also, in computing implementations of (19), only 182 terms or less need be computed for the summation; since early terms older than 182 days (with a constant aging function value) can be combined into a single term with some equivalent "replacement" age, then the first two terms of the summation in (19) can be replaced with the single term that uses the end-of-day heat storage of the second term ( $H_2$ ),  $H_0$ , and the replacement age. In general, the replacement age for the next day's oldest heat addition can be found from the present day's replacement age so that the oldest terms can be combined. Finally, note that any term in the summation in (19) that becomes zero,  $\min_{m \leq n \leq j} H_n - \min_{m-1 \leq n \leq j} H_n = 0$ , will always be zero on subsequent days; it can be eliminated from all further consideration whenever heat in storage drops below a past value.

Several aging functions and other variations of (17) were investigated including linear and exponential temperature difference terms, aging functions, and their combinations. Better proxies might be constructed for the aging function, especially since wind speed is available in the data set. However, (19) and (21) preserve essential features. Turnovers can occur as a fundamental behavior of (19) and (21). Hysteresis between  $H$  and  $T_w$  is present since the aging function increases with time. This implies more heat is stored or lost per degree change in surface temperature with age. A related effect is given by the temperature difference term power ( $c$  or  $c'$ ). For  $c$  (or  $c'$ ) smaller than unity, there is a bigger change in heat storage (or heat deficiency) per degree of surface temperature for lower surface temperatures than for higher ones (for  $c$  or  $c'$  greater than unity this is reversed). These two effects both give rise to types of hysteresis and are offsetting but related to different aspects of the process (time and temperature). Furthermore, each dominates at different parts of the process. The trade-off between these two effects is controlled of course by the values of the coefficients.

## HEAT BUDGET

### Fluxes Over Water

Heat in storage in the lake at the end of each day is given by a simple conservation of energy:

$$H_{j+1} = H_j + [(1 - I)A(Q_i - Q_r + Q_l - Q_e + Q_h + Q_p) + Q_l - Q_o]d + Q_m + o \quad (22)$$

where  $j$  is the number of the day for which the following fluxes apply,  $Q_i$ , the daily average rate of incident short-wave radiation to a unit area,  $Q_r$ , the daily average rate of short-wave radiation reflected from a unit area of surface,  $Q_l$ , the daily average rate of net long-wave radiation exchanged between the atmosphere and a unit area of surface,  $Q_e$  and  $Q_h$ , the daily average rates of latent and sensible heat transfers from a unit area, respectively,  $Q_p$ , the daily average energy advection rate into the lake by precipitation on a unit area of surface,  $Q_r$ , the daily average energy advection rate into the lake by runoff and river inflow,  $Q_o$ , the daily average energy advection rate out of the lake,  $d$ , the time in 1 day,  $Q_m$ , the correction to heat balance for the disappear-

ance of the ice cover during the day (since some of the energy flux computed over ice applies over water), and  $o$ , the other terms (including heat transfer through the bottom of the lake and energy advected with evaporation) which are neglected here.

The daily average incident short-wave radiation rate is taken here as

$$Q_i = [0.355 + 0.68(1 - N)]Q_o \quad (23)$$

where  $N$  is the cloud cover expressed as a fraction and  $Q_o$  is the daily average short-wave radiation rate received on a horizontal unit area of the Earth's surface under cloudless skies [Gray, 1973]. The daily average reflected short-wave radiation rate  $Q_r$  is taken here simply as one tenth of the incident, after Gray [1973], as an average for a water surface.

The daily net long-wave radiation exchange between the atmosphere and a water surface  $Q_l$  is derived from considerations of radiation from a water body and the atmosphere as affected by cloud cover. By considering a water body as a gray body, and by applying cloud cover corrections only to counter-radiation from a clear sky, the daily net long-wave radiation rate per unit of surface in watts per square meter is

$$Q_l = 5.67 \times 10^{-8} T_a^4 (0.53 + 0.065e_a^{1/2}) [p + (1 - p)(1 - N)] - 0.97 \cdot 5.67 \times 10^{-8} (T_w + 273.16)^4 \quad (24)$$

where  $5.67 \times 10^{-8}$  is the Stefan-Boltzmann constant (in watts per square meter per  $^\circ\text{K}$ ),  $T_a$  is the air temperature ( $^\circ\text{K}$ ),  $e_a$  is the vapor pressure of the air (mb) at the 2-m height,  $p$  is an empirical coefficient that reflects the effect of cloudiness on the atmospheric long-wave radiation to the Earth, 0.97 is the emissivity of water, and 273.16 is the freezing temperature in  $^\circ\text{K}$ . The expression in the first set of parentheses in (24) is for atmospheric emissivity after Keijman [1974], Kramer [1957], and U.S. Geological Survey [1954]. Most often, corrections are made to both atmospheric and water body radiation for cloud cover [Gray, 1973; Penman, 1948]. However, cloud cover affects atmospheric radiation and not the surface radiation; the correction is made only to the former in (24) after Keijman [1974].

The daily average rate of latent heat transfer  $Q_e$  is

$$Q_e = -r_w v E_w \quad (25)$$

where  $v$  is the latent heat of vaporization, and the daily average rate of sensible heat transfer  $Q_h$  is determined from (8), (9), (10), and (25) as

$$Q_h = BQ_e \quad (26)$$

where  $B$  is Bowen's ratio [Gray, 1973, equation III.19] evaluated for air and water temperatures and vapor pressures.

Energy advected with precipitation occurs at the rate

$$Q_p = r_w (CT_a - f)P \quad T_a < 0 \\ = r_w CT_a P \quad T_a \geq 0 \quad (27)$$

where  $f$  is the heat of fusion for water,  $P$  is the precipitation rate expressed as a depth per unit time, and  $T_a$  is in  $^\circ\text{C}$ . When the air temperature is below freezing, precipitation is considered as snow and the heat of fusion is removed from the surface as the snow melts. The energies advected into and out of the lake with other water flows occur at the rates of

$$Q_I = Rr_w CT_w \quad (28)$$

$$Q_O = Or_w CT_w \quad (29)$$

respectively, where  $R$  is runoff (from the basin to the lake) and river flow rates to the lake and  $O$  is river outflow rate from the lake, and  $T_w$  is in  $^\circ\text{C}$ .

#### Fluxes Over Ice

The heat delivered to the ice cover each day,  $H'$ , is given by a simple account of energy fluxes:

$$H' = IA(Q_i - Q_r' + Q_l - Q_e' + Q_h' + Q_p')d + o' \quad (30)$$

where  $Q_r'$  is the daily average rate of short-wave radiation reflected from a unit area,  $Q_l'$  is the daily average rate of net long-wave radiation exchanged between the atmosphere and a unit area,  $Q_e'$  and  $Q_h'$  are the daily average rates of latent and sensible heat transfers from a unit area of ice, respectively,  $Q_p'$  is the daily average energy advection rate onto a unit area by precipitation on the ice surface, and  $o'$ , the other terms ignored here as negligible. The daily average reflected short-wave radiation rate  $Q_r'$  is taken here as 45% of the incident for bare ice [Gray, 1973].

The daily net long-wave radiation exchange between the atmosphere and an ice surface  $Q_l'$  is found from (24); this is equivalent to ignoring the ice cover for net long-wave exchange with the atmosphere; ice cover probably does have some effect on the exchange, but the thermal radiation variation between open water and ice-covered water is ignored. The daily average rates of latent and sensible heat transfers from an ice surface,  $Q_e'$  and  $Q_h'$ , are

$$Q_e' = -r_w(v_l + f)E_l \quad (31)$$

$$Q_h' = B'Q_e' \quad (32)$$

respectively, where  $v_l$  is the latent heat of vaporization evaluated at the temperature of the ice surface  $T_I (= \min(T_a, 0))$  for temperatures in  $^\circ\text{C}$ ,  $f$  is the heat of fusion of water,  $E_l$  is the overice evaporation rate computed from (10) by using temperatures and specific humidities over ice, and  $B'$  is Bowen's ratio [Gray, 1973, equation III.19] evaluated with temperatures and specific humidities for the ice surface. Finally, energy advected with precipitation onto the ice surface occurs at the rate

$$Q_p' = r_w CT_a P \quad (33)$$

The heat delivered to the ice cover each day  $H'$  can be used to adjust the ice cover mass for accumulation, aggradation, and ablation,

$$M_2 = M_1 - H'/fr_i \quad H'/fr_i \leq M_1 \quad \text{and } I > 0 \\ = 0 \quad H'/fr_i > M_1 \quad \text{or } I = 0 \quad (34)$$

where  $M_1$  and  $M_2$  are the masses of the ice cover at the beginning and end of the day, respectively, and the heat correction to (22) for the disappearance of the ice cover during the day is

$$Q_m = H' - (M_1 - M_2)fr_i \quad (35)$$

The use of  $T_I = \min(T_a, 0)$  as ice surface temperature is an approximation that could conceivably be improved by keeping track of an ice temperature in the heat balance for the ice

cover; but with the uncertainties in the ice heat flux terms and especially in the evaluation of overice albedoes, such a calculation is inappropriate.

### Heat Balance

Given the heat storage at the beginning of the day (which is equal to that at the end of the previous day) and given daily overland wind speed, air temperature, cloud cover, and humidity and overlake precipitation, runoff, and inflows and outflows, then (1)–(14), (19) or (21), and (22)–(35) are solved simultaneously to determine heat storage at the end of the day, all heat fluxes, surface temperatures, and lake evaporation. Details of an iterative solution technique are available elsewhere [Croley, 1989]. Computation of surface temperatures is constrained to above-freezing temperatures even though the heat in the lake is allowed to drop below the amount corresponding to freezing surface temperatures on a given day. This represents a departure from the assumed heat storage of (21), possibly the result of additional ice formation not accounted for separately in the model. The energy is balanced in the model with surface temperatures held at freezing until sufficient heat is again in storage to allow surface temperatures to rise, possibly the result of additional ice melt not accounted for separately in the model.

## APPLICATION

### Calibration

Air temperature, wind speed, humidity, and cloud cover data for 1948–1985 were taken from 5 to 10 selected stations about each Great Lake (2 for Lake St. Clair) and averaged to determine daily overland meteorology to which overwater corrections can be applied [Croley, 1989]. Daily short-wave radiation under cloudless skies was interpolated from atmosphere-adjusted mid-monthly values available from stations near each lake [Gray, 1973]. Remotely sensed surface temperatures from (1) the National Oceanic and Atmospheric Administration's series of Polar Orbiting Satellites Advanced Very High Resolution Radiometers (for 1980 to present [Irbe and Saulesleja, 1982; Irbe et al., 1982; AES, 1988]) and (2) the Atmospheric Environment Service's airborne surveys of water surface temperatures (for 1966–1980 [Irbe, 1972]) were reduced for all Great Lakes except Michigan by the Hydrometeorology Division of AES. The Canadian Climate Centre currently uses the 10.5-micron infra red channel from both daily passes of both satellites and calculates atmospheric corrections from radiosonde data; they report a 0.5°C root-mean-square error between the satellite-derived temperatures and available buoy temperatures. The reported temperatures are instantaneous values obtained through interpretation of both visible light (for cloud and ice cover) and infrared pictures of the Great Lakes and may be higher than representative for a daily average. Since there is a larger diurnal range of surface temperatures during warm seasons, direct use of these instantaneous values may give evaporation estimates unrepresentative of daily average losses. Other problems include an imprecise knowledge of satellite locations, a fair weather bias (since daytime observations are used with clear or mostly clear skies, light winds, and an absence of steam fog on the lakes), and an avoidance of the split-channel technique of extracting surface temperatures (an empirical approach used widely for producing sea

surface temperatures globally), since it does not work well over land and lakes (G. J. Irbe, personal communication, 1988). However, these measurements form an independent set of data that may be used for comparisons in heat budget calculations.

The heat balance model is calibrated to determine values of the seven (7) parameters ( $a$ ,  $b$ ,  $c$ ,  $a'$ ,  $b'$ ,  $c'$ , and  $p$ ) with  $x = x' = 1$  that give the smallest sum-of-squared-errors between model and actual daily surface temperatures, observed remotely during a calibration period, similar to methods described elsewhere for calibrating rainfall runoff models [Croley and Hartmann, 1984]. Calibrations were performed over the last few data-rich years, 1978–1985, and were verified by comparison with the earlier years (1965–1977). No data were used until 1980 in the calibrations which allowed sufficient initialization. Marginal improvements were observed by setting  $x = 4$  and  $x' = 1$ . Calibration results are summarized in Table 3.

The goodness-of-fit statistics for the calibration and verification periods in Table 3 show generally good agreement on the deep lakes between the actual and calibrated model surface temperatures; correlations are high and means and variances are close between the data and model for each lake. The root mean square errors are 1.2°–1.5°C on the deep lakes. It was necessary to set parameter  $b$  to zero for the St. Clair and Erie calibrations; the minimum allowed by the calibration procedure,  $0.1 \times 10^{-9}$ , was still too big to be feasible on these shallow lakes. Note that the calibrated value of the exponent,  $c$  in (19) is the closest to unity for Lake Erie of all of the calibrations. This is consistent with shallow lake concepts in which the water throughout the depth is at the same temperature (and equal to the surface temperature) between spring and fall turnovers. The heat in the lake is described best then by a near-linear function of surface temperature.

Note that the goodness-of-fit for each lake, in terms of the root-mean-square error during the calibration period, varies inversely with the volume of the lake. This suggests that the heat storage superposition model is most applicable to the deep lakes and presumably fails on the shallower lakes where mechanical mixing of the shallow waters by winds is poorly represented by the aging function. However, other calibrations, not shown here, in which the black body long-wave radiating temperature was taken as a linear function of the heat in storage (2 additional parameters) and in which the lake evaporation coefficient was allowed to float (one additional parameter), gave a root-mean-square error on Erie of 1.2°C (there were little differences on the deep lakes). Unfortunately, there is little physical basis for those modifications and additional parameters; it is not possible to explain the improved goodness-of-fit nor to have much confidence in applying the resulting model to meteorologic conditions outside of those represented in the data set (such as various climate-change scenarios). Nevertheless, while the extra degrees of freedom allowed better matching of water surface temperatures, wind data were not utilized any more than in the present model. Conceptual model improvements may then be possible not only by considering wind data in improved mixing models for shallow lakes but also by considering changes in heat fluxes more appropriate for shallow lakes.

Of course, there are many sources for error including the model concepts for heat storage, heat balance, evaporation,

TABLE 3. Daily Calibration Results

|  | Lake                   |                        |                        |                        |                        |
|--|------------------------|------------------------|------------------------|------------------------|------------------------|
|  | Superior               | Huron                  | St. Clair              | Erie                   | Ontario                |
| Surface area, km <sup>2</sup>                                | 82,100                 | 59,600                 | 1,114                  | 25,700                 | 18,960                 |
| Volume, km <sup>3</sup>                                      | 12,100                 | 3,540                  | 3.3                    | 484                    | 1,640                  |
| Average depth, m   | 147                    | 59.4                   | 3.05                   | 18.8                   | 86.5                   |
| <i>Calibrated Parameter Values</i>                           |                        |                        |                        |                        |                        |
| $a$ , 10 <sup>20</sup> cal °C <sup>-c</sup>                  | $0.200 \times 10^{-1}$ | $0.105 \times 10^{-1}$ | $0.975 \times 10^{-4}$ | $0.421 \times 10^{-2}$ | $0.308 \times 10^{-2}$ |
| $b$ , day <sup>-4</sup>                                      | $0.381 \times 10^{-7}$ | $0.118 \times 10^{-7}$ | 0                      | 0                      | $0.110 \times 10^{-7}$ |
| $c$  | $0.981 \times 10^{+0}$ | $0.836 \times 10^{+0}$ | $0.930 \times 10^{+0}$ | $0.104 \times 10^{+1}$ | $0.899 \times 10^{+0}$ |
| $a'$ , 10 <sup>20</sup> cal °C <sup>-c</sup>                 | $0.376 \times 10^{-1}$ | $0.309 \times 10^{-1}$ | $0.716 \times 10^{-3}$ | $0.984 \times 10^{-2}$ | $0.431 \times 10^{-2}$ |
| $b'$ , day <sup>-1</sup>                                     | $0.200 \times 10^{-1}$ | $0.100 \times 10^{-9}$ | $0.100 \times 10^{-9}$ | $0.100 \times 10^{-9}$ | $0.312 \times 10^{-1}$ |
| $c'$   | $0.981 \times 10^{+0}$ | $0.987 \times 10^{+0}$ | $0.299 \times 10^{+1}$ | $0.823 \times 10^{+0}$ | $0.801 \times 10^{+0}$ |
| $p$  | $0.149 \times 10^{+1}$ | $0.133 \times 10^{+1}$ | $0.128 \times 10^{+1}$ | $0.157 \times 10^{+1}$ | $0.133 \times 10^{+1}$ |
| <i>Calibration Period Statistics (1979–1985)<sup>a</sup></i> |                        |                        |                        |                        |                        |
| Number of Observations                                       | 110                    | 165                    | 64                     | 150                    | 189                    |
| Means ratio <sup>b</sup>                                     | 1.05                   | 0.99                   | 1.09                   | 1.03                   | 0.98                   |
| Variances ratio <sup>c</sup>                                 | 0.95                   | 0.97                   | 1.34                   | 1.16                   | 0.98                   |
| Correlation <sup>d</sup>                                     | 0.98                   | 0.98                   | 0.97                   | 0.98                   | 0.98                   |
| RMSE <sup>e</sup>  | 1.20                   | 1.32                   | 2.81                   | 1.95                   | 1.48                   |
| <i>Verification Period Statistics (1966–1978)</i>            |                        |                        |                        |                        |                        |
| Number of observations                                       | 94                     | 160                    |                        | 104                    | 149                    |
| Means ratio <sup>b</sup>                                     | 0.95                   | 0.98                   |                        | 1.12                   | 1.05                   |
| Variances ratio <sup>c</sup>                                 | 1.11                   | 0.99                   |                        | 1.42                   | 1.02                   |
| Correlation <sup>d</sup>                                     | 0.93                   | 0.98                   |                        | 0.97                   | 0.98                   |
| RMSE <sup>e</sup>  | 1.62                   | 1.26                   |                        | 2.76                   | 1.57                   |
| <i>Combined Period Statistics (1966–1985)</i>                |                        |                        |                        |                        |                        |
| Number of observations                                       | 204                    | 325                    | 64                     | 254                    | 338                    |
| Means ratio <sup>b</sup>                                     | 1.00                   | 0.99                   | 1.09                   | 1.07                   | 1.01                   |
| Variances ratio <sup>c</sup>                                 | 1.00                   | 0.97                   | 1.34                   | 1.25                   | 0.99                   |
| Correlation <sup>d</sup>                                     | 0.96                   | 0.98                   | 0.97                   | 0.97                   | 0.98                   |
| RMSE <sup>e</sup>  | 1.41                   | 1.29                   | 2.81                   | 2.31                   | 1.52                   |

<sup>a</sup>Data between January 1, 1979, and December 31, 1985, for all Great Lakes and between January 1, 1979, and December 31, 1983, for Lake St. Clair.

<sup>b</sup>Ratio of mean model surface temperature to data mean.

<sup>c</sup>Ratio of variance of model surface temperature to data variance.

<sup>d</sup>Correlation between model and data surface temperature.

<sup>e</sup>Root-mean-square error between model and data surface temperatures in °C.

ice cover, overwater corrections, the satellite observations themselves, and the overland meteorological data at stations about each lake. The good agreement between model and observations is no doubt partially due to somewhat compensating errors.

Figure 1 contains surface temperatures calculated with the Lake Ontario application of the model calibration summarized in Table 3, as applied to historical meteorological data over the calibration and verification periods. Lake Ontario was chosen for display since it is the poorest fit among the deep Great Lakes and the others show better agreement with the data. Inspection of Figure 1 reveals that turnover is predicted within about 1–2 weeks most of the time; above-freezing winters are replicated (as much as can be seen from the scanty data) most of the time; late summer peaks in surface temperature appear poorly duplicated (when there are data at those times) with the model consistently under-

estimating them. However, this latter observation is consistent with the recognized fair weather and day time bias to the data and with the higher diurnal range of surface temperatures that exists during periods of high temperatures.

#### *Evaporation and Heat Fluxes*

The estimation of water surface temperatures enables the calculation of all components of the heat balance including evaporation. Figure 2 compares the model output for April 1972 through March 1973 (data wraps around the calendar year in Figure 2) to Lake Ontario heat fluxes measured during IFYGL by Schertzer [Pinsak and Rodgers, 1981]. Another data comparison for Lake Ontario and comparisons for Superior and Erie are available elsewhere [Croley, 1989] and the results are similar to those shown here. Sensible, latent, and net radiation fluxes are well represented. The large peak in latent flux in July (and the corresponding peak

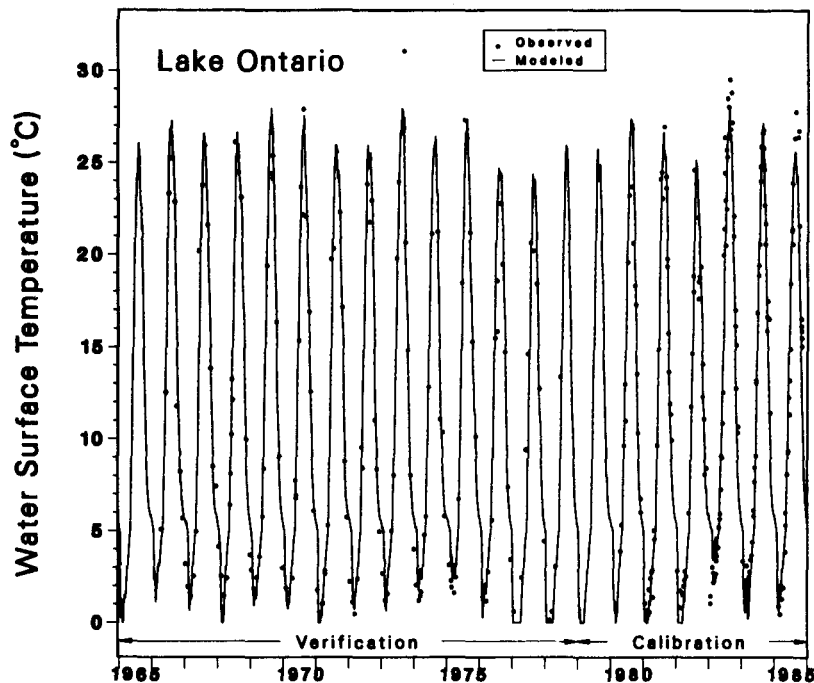


Fig. 1. Lake Ontario water surface temperature.

in sensible flux) appears anomalous; it is not present in an estimate by Atwater [Pinsak and Rodgers, 1981]. Several of the heat flux concepts used by the others [Pinsak and Rodgers, 1981; Schertzer, 1978, 1987] are similar to those used here, but all data used by these investigators are completely independent of the data used here, representing independent estimates of the heat budget terms.

Figure 2 shows the modeled net radiation flux and its good agreement with measurements but does not indicate the agreement of the components on the net radiation flux: incident, reflected, and long wave. These components are shown elsewhere [Croley, 1989], revealing that modeled net long-wave radiation is often positive during the summer months on Lakes Superior and Erie; that is, long-wave radiation from the atmosphere to the lake (first term in equation (24)) is then greater than long-wave radiation from the lake to the atmosphere (second term in equation (24)). This is not in accord with current thinking for these lakes but may be the result of parameter compensation in the model calibrations; note that parameter  $p$  is higher on lakes Superior and Erie in Table 3. Keijman [1974] used  $p = 1.13$ , for a small lake near Amsterdam, which is lower than that used here for any of the Great Lakes. Perhaps atmospheric long-wave radiation is overestimated in the model to compensate for deficiencies in other modeled heat flux components. Further model analysis and consideration of measurements are necessary to understand the opportunity for parameter compensation in the model calibrations, the relevancy of the atmospheric long-wave radiation flux term in (24), and the omission of important concept components in the other heat budget terms in (22).

Evaporation is strongest in the fall and winter on the Great Lakes. Evaporation peaks on all lakes in September and again on the deep lakes during December or January. While the two evaporation peaks are reflected in the latent flux in the 1 year of data in Figure 2, they are also present in long-term averages for all deep lakes. The first peak results

from the high surface temperatures and dropping humidities that occur in the fall. On the deeper lakes, this effect lasts into the winter as surface temperatures drop more slowly. The second peak occurs on the deep lakes due to the winter drop in humidity in the overlying air, coupled with higher wind speeds and mass transfer in the air column. Furthermore, shorter-term fluctuations in evaporation are tied to like changes in wind speed and, to a lesser extent, net long-wave radiation. Large amounts of evaporation also occur on an episodic basis corresponding to high winds and dry air. Evaporation events occur on all lakes but are most pronounced on Lake Superior during the winter when cold dry air masses cross the lake quickly. Advection is very small on all lakes and generally can be neglected. Thus knowledge of precipitation, runoff, and other lake inflows and outflows is not essential for use of the models in calibration, simulation, or forecast settings. During the winter, energy for the losses comes from the large heat storage built during the summer and fall when evaporation is lower. The total heat flux budget over 1950–1985 appears to close (there is no average annual residual in the budget over this period) with as much energy outgoing as incoming over the annual cycle; since the average represents 36 years, little carryover is expected. Large residuals noted in earlier heat budgets [Schertzer, 1978] that are avoided only when evaporation is estimated as the heat budget residual are minimized here by calibration of the flux models and heat storage function to best match surface temperatures.

#### Water Balance Residuals

A comparison with water balance evaporation estimates [Croley, 1989] reveals annual differences on Lake Ontario for the period 1965–1985 of  $50\text{--}150\text{ m}^3\text{ s}^{-1}$  (1–3% of the average flow) and may be partially related to flow determination errors. Lake Superior annual residuals are  $50\text{--}150\text{ m}^3\text{ s}^{-1}$  and may be related to improper consideration of a diversion into the lake. Lake St. Clair annual residuals were

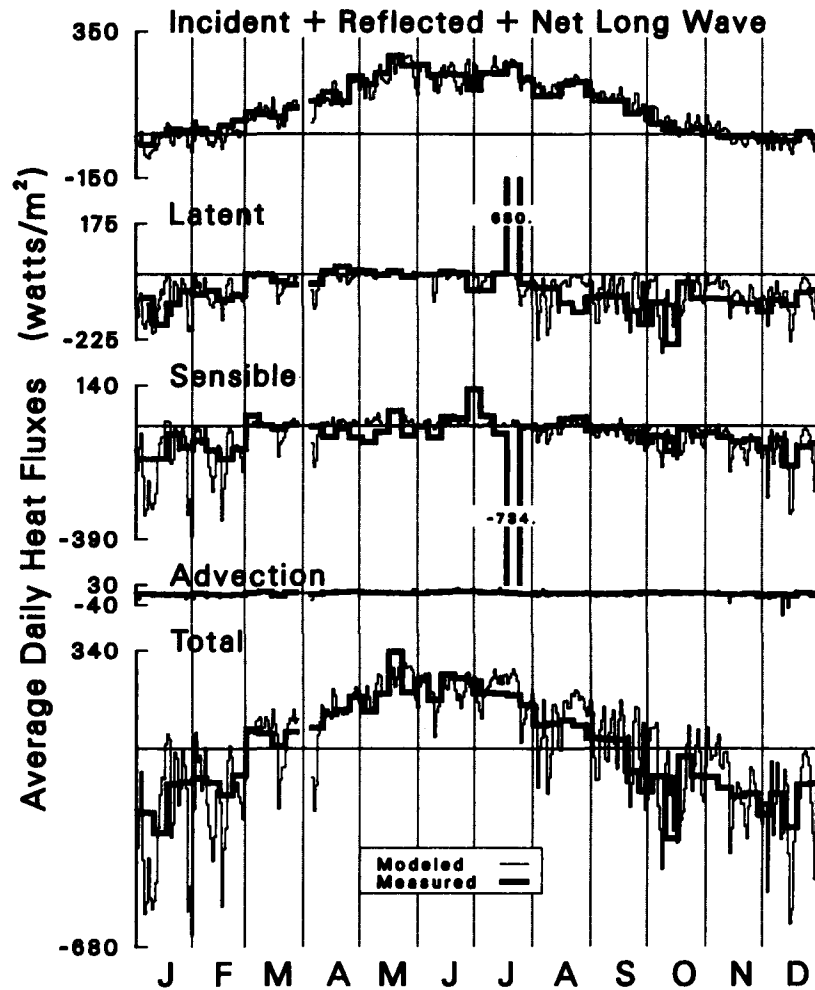


Fig. 2. IFYGL (April 1972 to March 1973) Lake Ontario fluxes comparisons.

only  $50 \text{ m}^3 \text{ s}^{-1}$  and Lake Erie annual residuals were consistently negative on the order of  $100\text{--}200 \text{ m}^3 \text{ s}^{-1}$ , suggesting a problem with the estimation of evaporation or of the other mass balance components on that lake. Operational evaporation estimates that also use the aerodynamic equation with a stability-dependent mass transfer coefficient but applied directly to estimated surface temperatures [AES, 1988] gave larger annual residuals on all lakes (except Erie) that may result from errors in observed surface temperatures and data reductions which are filtered here by the minimization of the root mean square error in the calibrations of the heat budget and heat storage models. In the earlier calibration, mentioned under "Calibration," where the evaporation mass transfer coefficient was allowed to float in the calibrations and the long-wave radiating temperature was taken as a linear function of the heat in storage, much better agreement on Lake Erie was observed with AES evaporation estimates in addition to better matches of satellite-observed surface temperatures. While there is little physical basis for these extra degrees of freedom in the model, their net effect was to provide more heat release through long-wave radiation than through evaporation. The present model of Table 3 appears to overestimate evaporation when compared to mass balance estimates or to the AES estimates. Part of the problem may be in poor estimates of the mass balance components but both the AES estimate and the present model should be

close, since the evaporation calculations are very similar. The difference might lie in AES's adjustment of temperature data to incorporate normal seasonal surface temperature variations or in the different set of meteorological stations used. Further analysis of the energy and mass balances and of alternate approaches are required to assess these discrepancies on Lake Erie.

#### Model Sensitivities

Sensitivity studies [Croley, 1989] reveal that evaporation and surface temperature estimates are most sensitive to the cloud cover parameter  $p$ , which controls the net long-wave radiation received. Evaporation on the deep lakes rises about  $1 \text{ cm/year}$  as  $p$  is increased by 1%, and  $1\frac{1}{2}$  to  $1\frac{3}{4} \text{ cm/year}$  on the shallower lakes. Evaporation sensitivities to the heat storage parameters vary from lake to lake with the exception of parameter  $c$ . Small changes in this exponent can give large changes in heat storage per degree of temperature rise. The careful selection of this parameter allows mimicry of some aspects of the hysteresis present between heat in storage and surface temperature over the annual heating and cooling cycle. It appears that applications of the heat balance, heat storage, and evaporation models described here to other lakes without surface temperatures available, such as Lake Michigan, will require careful selec-

tion particularly of  $a$ ,  $c$ , and  $p$  and generally of  $b$ ,  $a'$ ,  $b'$ , and  $c'$ .

#### SUMMARY

Available remotely sensed water surface temperatures enable the calibration of a joint evaporation–heat balance–heat storage daily model; such calibrations are not possible in terms of matching measured evaporation, since independent evaporation estimates do not exist for the Great Lakes or are too crudely determined in energy or water balances. Traditional heat flux expressions are combined with current use of the aerodynamic (evaporation) equation, with mass transfer coefficients determined from stability considerations, and used with a new lumped model of superposition heat storage in a lake. This enables modeling of surface temperature as well as evaporation which makes the model amenable to use in continuous simulation settings where surface temperatures are unknown, including forecasts, climate change simulations, and assessments of management impacts on the hydrology of the Great Lakes.

The heat storage model is a superposition model where the latest heat additions to the lake are the first removed. While, conceptually, heat losses actually come from some mix of past heat additions, this model allows aging of heat additions to be considered that describe well the observed hysteresis between stored heat and surface temperature. Alternate aging functions, perhaps as functions of wind history, may better describe the maturation of the heat distribution in a lake and this is an area for future research with lumped heat storage models.

The new heat storage model, when used with contemporary treatments of evaporation and heat exchange, appears to do a good job of replicating average areal surface temperatures and heat fluxes on the deep lakes. Correlations between model and remotely observed average areal surface temperatures are 0.97–0.99 during the calibration period of 1979–1985 and range from 0.93 to 0.98 during a verification period of 1966–1978. The corresponding root-mean-square errors are 1.2°–1.5°C for the calibrations and 1.3°–1.6°C for the verification periods. These errors compare favorably with reported accuracies for reduction of remotely sensed data. On the shallow lakes, greater errors in surface temperature are observed in the calibrations. On Lake Erie, it appears that resulting evaporation may also be overestimated. Future research can address alternate heat flux formulations, wind-induced mixing (aging) functions, and heat storage models more appropriate for shallow lakes. Inspection of model outputs reveals that significant aspects of the annual heating and cooling cycle in each Great Lake are replicated including the spring and fall turnovers, near-peak daily average surface temperatures, and above-freezing winter surface temperatures. Resulting heat fluxes agree very well with independent data sets used by other investigators, where available, for Lakes Superior, Erie, and Ontario, with the possible exception of atmospheric long-wave radiation; further work is necessary to see if overestimation of this exists and results from parameter compensation in the model calibrations and then to see what other terms are being compensated.

These evaporation estimates result in water balance residuals which are largest on Lake Erie and may be related to neglected water balance terms (such as groundwater), systematic errors of measurement of river inflows, and outflows

and runoff, and/or process model errors in the evaporation. This is an area for further research as these residuals must be considered for simulations of climate change or management impacts on lake levels or for forecasting of lake levels. While the nature of the residuals is unresolved at present, comparisons with conventional evaporation models that directly use observed surface temperatures indicate that residuals are reduced by considering the heat exchange and heat storage in each deep lake.

Other areas for further research include improvements to the models in the areas of ice cover estimation, incorporation of better ice cover thermodynamics into the heat balance, estimation of ice cover effects on heat fluxes (notably long-wave exchange and reflection), and better assessment of overwater corrections to overland meteorology.

#### NOTATION

|                        |   |
|------------------------|---|
| $a$                    | empirically derived heat storage parameter, $T_w > 3.98^\circ\text{C}$ .      |
| $a'$                   | empirically derived heat storage parameter, $T_w \leq 3.98^\circ\text{C}$ .   |
| $a_1, a_2, a_3, a_4$   | empirical coefficients for bulk evaporation coefficient determination.        |
| $A$                    | area of the lake surface.   |
| $A(Z)$                 | area of water surface at height $Z$ .   |
| $b$                    | empirically derived heat storage parameter, $T_w > 3.98^\circ\text{C}$ .      |
| $b'$                   | empirically derived heat storage parameter, $T_w \leq 3.98^\circ\text{C}$ .   |
| $b_0, b_1, \dots, b_9$ | empirical coefficients for correction of meteorology to overwater conditions. |
| $B$                    | Bowen ratio.  |
| $B'$                   | Bowen ratio over ice.   |
| $c$                    | empirically derived heat storage parameter, $T_w > 3.98^\circ\text{C}$ .      |
| $c'$                   | empirically derived heat storage parameter, $T_w \leq 3.98^\circ\text{C}$ .   |
| $c_1, c_2, c_3$        | empirical ice coefficients on monthly air temperature.                        |
| $C$                    | specific heat of water.   |
| $C_E$                  | bulk evaporation coefficient.   |
| $C_H$                  | sensible heat coefficient.  |
| $C_p$                  | specific heat of air at constant pressure.                                    |
| $d$                    | time in 1 day.  |
| $D$                    | overwater dew point temperature.  |
| $D_1$                  | overland dew point temperature.   |
| $e_a$                  | vapor pressure of the atmosphere at the 2-m height.                           |
| $E_I$                  | evaporation over ice.   |
| $E_w$                  | evaporation over water.   |
| $f$                    | heat of fusion for water.   |
| $g$                    | acceleration due to gravity.  |
| $H'$                   | heat delivered to the ice cover each day.                                     |
| $H_d$                  | heat in storage at turnover.  |
| $H_j$                  | heat in storage in the lake at the end of day $j$ .                           |
| $I$                    | average monthly fraction of the surface covered by ice.                       |
| $k$                    | von Karmán's constant.  |
| $L$                    | Monin-Obukhov length.   |
| $M_1, M_2$             | masses of the ice cover at the beginning and end of the day, respectively.    |

- $N$  cloud cover expressed as a fraction.
- $o$  neglected terms in heat balance for a lake.
- $o'$  neglected terms in the ice cover heat balance.
- $O$  river flow rate from the lake.
- $p$  an empirical coefficient that reflects the effect of cloudiness on the atmospheric long-wave radiation to the Earth.
- $P$  precipitation rate expressed as a depth per unit time.
- $q$  specific humidity of the atmosphere.
- $q_w$  saturation specific humidity at the surface temperature.
- $Q_I$  daily average energy advection rate into a lake by runoff and river inflow.
- $Q_O$  daily average energy advection rate out of a lake.
- $Q_P$  daily average energy advection rate into a lake by precipitation on a unit surface area.
- $Q'_P$  daily average energy advection rate onto a unit surface area by precipitation on the ice.
- $Q_d$  daily average long-wave radiation rate from the atmosphere.
- $Q_e$  daily average rate of latent heat transfer from a unit water surface area.
- $Q'_e$  daily average rate of latent heat transfer from a unit ice surface area.
- $Q_h$  daily average rate of sensible heat transfer from a unit water surface area.
- $Q'_h$  daily average rate of sensible heat transfer from a unit ice surface area.
- $Q_i$  daily average rate of incident short-wave radiation to a unit surface area.
- $Q_l$  daily average rate of net long-wave radiation exchanged between the atmosphere and a unit water surface area.
- $Q'_l$  daily average rate of net long-wave radiation exchanged between the atmosphere and a unit ice surface area.
- $Q_m$  correction to heat balance for the disappearance of the ice cover during the day.
- $Q_r$  daily average rate of short-wave radiation reflected from a unit water surface area.
- $Q'_r$  daily average rate of short-wave radiation reflected from a unit ice surface area.
- $Q_u$  daily average long-wave radiation rate from a unit area of water surface.
- $Q_o$  daily average short-wave radiation rate received on a horizontal unit area of the Earth's surface under cloudless skies.
- $r$  air density.
- $r_w$  density of water.
- $r_i$  density of ice.
- $R$  runoff from the basin to the lake and river flow rates to the lake.
- $S_1$  stability-dependent parameter for the wind profile.
- $S_2$  stability-dependent parameter for the temperature profile.
- $T$  potential temperature at reference height.
- $T_*$  a scaling temperature.
- $T_a$  overland air temperature.
- $T'_a$  air temperature in °K.
- $T_d$  temperature of maximum water density.
- $T_j$  surface temperature ( $T_w$ ) at the end of day  $j$ .
- $T_w$  potential temperature at  $Z_w$ .
- $T_I$  temperature of the ice surface.
- $U$  mean wind speed at reference height  $Z$  above the surface.
- $U_*$  friction velocity.
- $v$  latent heat of vaporization.
- $v_I$  latent heat of vaporization evaluated at the temperature of the ice.
- $W$  overland wind speed.
- $x$  empirically derived parameter.
- $x'$  empirically derived parameter.
- $y$  heat penetration depth below water surface.
- $Z$  reference height above water surface.
- $Z_w$  roughness length.
- $Y$  absolute temperature of near-surface air.
- $Y_a$  average monthly overland air temperature.
- $Y_{a-1}$  average monthly overland air temperature for previous month.

*Acknowledgment.* GLERL contribution 631.

#### REFERENCES

- Assel, R. A., A computerized ice concentration data base for the Great Lakes, *NOAA Data Rep. ERL GLERL-24*, Environ. Res. Lab., Natl. Ocean. Atmos. Admin., Ann Arbor, Mich., 1983.
- Atmospheric Environment Service (AES), Monthly and annual evaporation from the Great Lakes bordering Canada, report Atmos. Environ. Serv., Environ. Canada, Downsview, Ont., 1988.
- Businger, J. A., Transfer of momentum and heat in the planetary boundary layer, in *Proc. Symp. Arctic Heat Budget and Atmos. Circul.*, pp. 305-331, The RAND Corporation, Santa Monica, Calif., 1966.
- Charnock, H., Wind stress on a water surface, *Q. J. R. Meteorol. Soc.*, *81*, 639-640, 1955.
- Croley, T. E. II, Lumped modeling of Laurentian Great Lakes evaporation, heat storage, and energy fluxes for forecasting and simulation, *NOAA Tech. Memo. ERL GLERL-70*, Environ. Res. Lab., Natl. Ocean. Atmos. Admin., Ann Arbor, Mich., 1989.
- Croley, T. E. II, and H. C. Hartmann, Lake Superior basin runoff modeling, *NOAA Tech. Memo. ERL GLERL-50*, Environ. Res. Lab., Natl. Ocean. Atmos. Admin., Ann Arbor, Mich., 1984.
- Derecki, J. A., Operational estimates of Lake Superior evaporation based on IFYGL findings, *Water Resour. Res.*, *17*(5), 1453-1462, 1981.
- Gill, A. E., and J. S. Turner, A comparison of seasonal thermocline models with observation, *Deep Sea Res.*, *23*, 391-401, 1976.
- Gray, D. M., G. A. McKay, and J. M. Wigham, Energy, evaporation, and evapotranspiration, *Handbook on the Principles of Hydrology*, edited D. M. Gray, Water Information Center, New York, 1973.
- Irbe, J. G., An operational program for measuring surface water temperature by airborne radiation thermometer [ART] survey, in *Proceedings First Canadian Symposium on Remote Sensing*, pp. 183-200, Atmospheric Environment Service, Department of the Environment, Downsview, Ont., 1972.
- Irbe, J. G., and A. Saulesleja, An operational program for monitoring surface temperatures of lakes and coastal-zone waters in Canada from Polar-orbiting satellite infrared data, *Actes du sym-*

- posium international de la Commission VII de la Societe internationale de photogrammetrie et teledetection, 13-17 September, Toulouse, France, *Int. Arch. Int. Soc. Photogram. Remote Sens.*, 24(VII-1), 717-724, 1982.
- Irbe, J. G., R. K. Cross, and A. Saulesleja, Remote sensing of surface water temperature of the Great Lakes and off the Canadian east coast, Northwest Atlantic Fisheries Organization Scientific Council Studies No. 4, paper presented at Special Session on Remote Sensing, Dartmouth, Canada, September 1982.
- Keijman, J. Q., The estimation of the energy balance of a lake from simple weather data, *Boundary Layer Meteorol.*, 7, 399-407, 1974.
- Kramer, C., Computation of the mean evaporation for various parts of the Netherlands according to Penman's method, *Kon. Ned. Meteor., Inst. Med. Verh.*, 70, 1957.
- Kraus, E. B., and J. S. Turner, A one-dimensional model of the seasonal thermocline, II, The general theory and its consequences, *Tellus*, 19, 98-105, 1967.
- Panofsky, H. A., Determination of stress from wind and temperature measurements, *Q. J. R. Meteorol. Soc.*, 89, 85-94, 1963.
- Paulson, C. A., The mathematical representation of wind speed and temperature profiles in the unstable atmospheric surface layer, *J. Appl. Meteorol.*, 9, 857-861, 1970.
- Penman, H. L., Natural evaporation from open water, bare soil and grass, *Proc. R. Soc. London., Ser. A*, 193, 120-145, 1948.
- Phillips, W. D., Evaluation of evaporation from Lake Ontario during IFYGL by a modified mass transfer equation, *Water Resour. Res.*, 14(2), 197-205, 1978.
- Phillips, W. D., and J. G. Irbe, Land-to-lake comparison of wind, temperature, and humidity on Lake Ontario during the International Field Year for the Great Lakes (IFYGL), *Rep. CLI-2-77*, Atmos. Environ. Serv., Environ. Canada, Downsview, Ont., 1978.
- Pinsak, A. P., and G. K. Rodgers, Energy balance, *IFYGL—The International Field Year For The Great Lakes*, edited by E. J. Aubert and T. L. Richards, pp. 169-197, National Oceanic and Atmospheric Administration, Ann Arbor, Mich., 1981.
- Quinn, F. H., An improved aerodynamic evaporation technique for large lakes with application to the International Field Year for the Great Lakes, *Water Resour. Res.*, 15(4), 935-940, 1979.
- Quinn, F. H., and R. K. Kelley, Great Lakes monthly hydrologic data, *NOAA Data Rep. ERL GLERL-26*, 1983.
- Richards, T. L., and J. G. Irbe, Estimates of monthly evaporation losses from the Great Lakes, 1950 to 1968, based on the mass transfer technique, paper presented at the 12th Conference on Great Lakes Research, Int. Assoc. of Great Lakes Res., Ann Arbor, Mich., May 1969.
- Schertzer, W. M., Energy budget and monthly evaporation estimates for Lake Superior, 1973, *J. Great Lakes Res.*, 4(3-4), 320-330, 1978.
- Schertzer, W. M., Heat balance and heat storage estimates For Lake Erie, 1967 to 1982, *J. Great Lakes Res.*, 13(4), 454-467, 1987.
- U.S. Geological Survey, Water loss investigations, Lake Hefner studies, *U.S. Geol. Surv. Prof. Pap.*, 269, 1954.
- U.S. Geological Survey, Water loss investigations: Lake Mead studies, *U.S. Geol. Surv. Prof. Pap.*, 298, 1958.
- T. E. Croley II, Great Lakes Environmental Research Laboratory, Environmental Research Laboratories, National Oceanic and Atmospheric Administration, U.S. Department of Commerce, 2205 Commonwealth Boulevard, Ann Arbor, MI 48105.

(Received September 27, 1988;  
revised January 26, 1989;  
accepted January 31, 1989.)